Available online at www.sciencedirect.com
ScienceDirect
Electrochimica Acta 53 (2007) 664–672
ELECTROCHIMICA Acta
www.elsevier.com/locate/electacta

Palladium electrodeposition on polyaniline films

A. Mourato [a,b], J.P. Correia [a], H. Siegenthaler [b], L.M. Abrantes [a,*]

[a] *Departamento de Química e Bioquímica da Faculdade de Ciências da Universidade de Lisboa, Campo Grande, 1749-016 Lisboa, Portugal*
[b] *Department of Chemistry and Biochemistry, University of Bern, Freiestrasse 3, CH-3012 Bern, Switzerland*

Received 21 June 2007; received in revised form 13 July 2007; accepted 14 July 2007
Available online 28 July 2007

Abstract

The electrochemical nucleation and growth of palladium particles onto polyaniline (PAni) films have been investigated by chronoamperometry and topographic and phase-mode atomic force microscopy (AFM). The films were synthesized under different potentiodynamic conditions in order to obtain polymer layers with comparable electroactivity but distinctly different morphology/porosity. The analysis of the current transients obtained for the initial stages of the Pd deposition indicates a 3D nucleative formation regime. A detailed Pd electrodeposition study onto the polymer matrix, using different deposition times, suggests that a constant number of critical nuclei is formed in the superficial part of the polymer porous matrix in the time scale between ca. 5 and 15 s.

Keywords: Polyaniline; Palladium; Electrodeposition; AFM

1. Introduction

Metal micro/nanoparticles are intensely studied due to their unique optical, electrical and catalytic properties. The special properties of sub-microparticles are due to their large surface area, which is related with their size, distribution, exposed surface area structure and mode of preparation in the dispersing medium [1–6]. To utilize and optimize the chemical/physical properties of nanosized metal particles, a large amount of research has focused on the control of the size and shape.

Conducting polymers can be used as proper host matrices to obtain highly dispersed metallic particles and have been subject of great scientific interest since different and sometimes novel properties are obtained as compared with bulk materials [1,7,8]. In particular, metal microparticles dispersed in polymer modified electrodes have been recognized to have potential applications in electrocatalysis. Many research groups have studied the incorporation of metal microparticles (e.g. Pt, Pd) particles in polyaniline (PAni) matrices in order to enhance the electrocatalytic activity as compared with the bulk-form metal electrodes [2,5,7,9–13]. As a conducting polymer substrate, PAni is one of the most attractive polymers on account of its high conductivity, stability in ambient conditions, easy polymerisation and for its multiple oxidation and protonation states [14]. Another important feature is that PAni films present a high surface area due to the high porosity of the films formed by various methods [15,16]. The electrochemical polymerisation provides the possibility of controlling the thickness, homogeneity and morphology of the polymer film on the electrode surface [10,17]. There are different methods for the deposition of Pd particles on the polymer matrix; most published studies are related to metal electrodeposition [18,19], co-deposition [18] and electroless precipitation [20–22]. In order to synthesise well-defined highly dispersed metal nanoparticles, control over the nucleation and growth process is essential. A suitable electrochemical method is the electrodeposition, since the growth conditions can be directly monitored with the applied potential and deposition time. Nevertheless, if the electrodeposition of noble metals is carried out into/onto PAni layers, it should be performed in such a way that no electroless precipitation of the metal particles occurs in the initial stages. This process arises when spontaneous polymer oxidation takes place with simultaneous reduction of the noble metal ion, provided that the reduction potential is in

* Corresponding author at: Dep. Química e Bioquímica da FCUL, Edifício C8, Campus da FCUL, Campo Grande, 1749-016 Lisboa, Portugal. Tel.: +351 21 7500000x28342; fax: +351 21 7500088.
E-mail address: luisa.abrantes@fc.ul.pt (L.M. Abrantes).

0013-4686/$ – see front matter © 2007 Elsevier Ltd. All rights reserved.
doi:10.1016/j.electacta.2007.07.050

the range where the conversion of the oxidised forms of PAni occurs [10,11].

In an earlier work [10], the present authors have shown that it is possible to obtain palladium nanoparticles on the polyaniline layers by electroless precipitation. Compact films were obtained with a slow electropolymerisation sweep rate, and the electrolessly deposited Pd clusters were of different sizes (80–200 nm and ~20 nm) and uniformly dispersed on the top of the polymer layer. In contrast, heterogeneous and porous films were obtained with a faster sweep rate of 60 mV/s. In this case, the results obtained by AFM demonstrated that the PAni nodules were apparently covered by a large amount of Pd particles of approximately 15 nm diameter, and SEM data also showed the presence of palladium clusters with diameters of 100–200 nm.

Given the current interest devoted to these modified electrodes, the aim of the present work was to evaluate the role of the polymer synthesis conditions, and ultimately of the structural properties of the PAni films, on the dispersion and size of the potentiostatically deposited palladium on/in a polymeric matrix.

2. Experimental

The PAni films were electropolymerised on polycrystalline gold electrodes in a 0.1 M solution of aniline in 0.5 M H_2SO_4 as described previously [10], by cycling the potential between −0.200 V and +0.800 V versus SCE for the first five cycles, then lowering the anodic limit to 0.750 V for the next three cycles, and to 0.70 V after eight cycles. The electrolyte solution was prepared with Milli-Q water from sulfuric acid (100%, Merck, for conductivity measurements) and from freshly distilled aniline stored under N_2 atmosphere. Polycrystalline gold disks ($A = 0.50\,cm^2$, purity 99.99%) were used as working electrodes and hand-polished in an aqueous suspension of successively finer grades of alumina (down to 0.05 μm) until a fresh mirror-finish surface was generated. A saturated calomel electrode (SCE) and a Pt foil were used as reference and counter electrodes, respectively, in a three-compartment cell.

Two different polyaniline film types were prepared by applying 17 polymerisation cycles at a potential sweep rate $v = 0.01$ V/s (17/10 films) and 200 polymerisation cycles at $v = 0.06\,s^{-1}$ (200/60 films). Prior to all measurements, the solutions were deaerated with N_2 for 15 min. The films were washed with Milli-Q water and electrochemically characterised in the electrolyte solution (monomer free solution) by cycling the potential between −0.200 and +0.400 V versus SCE at $v = 0.05$ V/s. The electrode potential was initially kept at −0.200 V for 10 min in order to completely discharge the film.

The synthesised PAni modified electrodes were used as substrates for the palladium electrodeposition.The polymer film, in its oxidised state, was transferred in the shortest lapse of time to the solution of 0.001 M $PdSO_4$ (98%, Aldrich) in 0.5 M H_2SO_4 where it was kept at +0.400 V versus SCE for 1 s. This procedure was done in order to avoid the electroless precipitation of palladium in/on the polymer film. The potential was then stepped to +0.120, +0.150 V or +0.190 V versus SCE, and the current transients recorded for 30 s (for $E = +0.120$ V), 60 s (for $E = +0.150$ V, $E = +0.190$ V), and for 1200 s and 1860 s (for $E = +0.190$ V), the last ones corresponding to deposition charges of ~15 mC cm^{-2} and ~33 mC cm^{-2}, respectively. Blank transients of the PAni films measured in Pd-free 0.5 M H_2SO_4 solutions were also performed.

The equipments used for the electrochemical experiments were a set-up consisting of a home-made potentiostat, a Waveform Generator PP R1 (Hi-Tek Instruments, England) and a Recorder X–Y Model 200 (The Recorder Company) for the potentiodynamic growth of the polyaniline films and for the potentiostatic deposition of palladium for 1200 and 1860 s ($E = +0.190$ V), and EG&G Princeton Applied Research (Model 473A) used for the palladium electrodeposition when pulse potentials of 30 and 60 s were applied.

The morphology of the modified electrodes was examined by Atomic Force Microscopy in the Tapping Mode, using a Nanoscope IIIa Multimode Atomic Force Microscope (Digital Instruments) equipped with the Extended Electronics Module for simultaneous topographic and phase imaging. Etched silicon tips, with ~300 kHz resonance frequency, were used as AFM probes.

The estimation of the visible amount of electrodeposited Pd was performed by the statistical analysis of the topographic and phase AFM images, by counting the features associated with Pd particles.

3. Results and discussion

3.1. Electrodeposition of palladium at polyaniline films

Potential-step has been used to investigate the palladium electrodeposition on/in the two previously described distinct types of polymer films (17/10 and 200/60). Systematic studies (not presented) were performed using a palladium electrode and polyaniline films as substrates to establish and select the palladium deposition potential in acidic solutions. The potential of a bulk palladium electrode in the 0.001 M $PdSO_4$ solution in 0.5 M H_2SO_4 is $E_{oc} = +0.550$ V versus SCE, and the electrodeposition of palladium on this substrate occurs at +0.300 V versus SCE. Taking into account this potential and the requirement to apply an overpotential, the electrodeposition of Pd in/on the polymer films was performed by applying a step potential from +0.400 to +0.190 V versus SCE, where PAni remains in the oxidised state (dashed line in the cyclic voltammograms shown in Fig. 1).

Fig. 2 displays the current transients obtained for the potentiostatic Pd deposition on both PAni films. At the initial potential the PAni films are in the polyemeraldine form (i.e., equal numbers of repetitive benzenoid and quinoid units) which corresponds to a maximum of conductivity, and when the potential step is applied, e.g. to 0.190 V versus SCE, the polymer matrix is also slightly reduced (Fig. 1, dashed line). Hence, under these conditions it should be expected, as reported in the literature [23–28], that the metal deposition occurs mainly on the top of the film surface since the polymer matrix is mostly in the conducting state. However, it cannot be excluded that some nucleation and growth of the metallic nuclei also takes place across the porous matrix and at the polymer film and metal substrate interface.

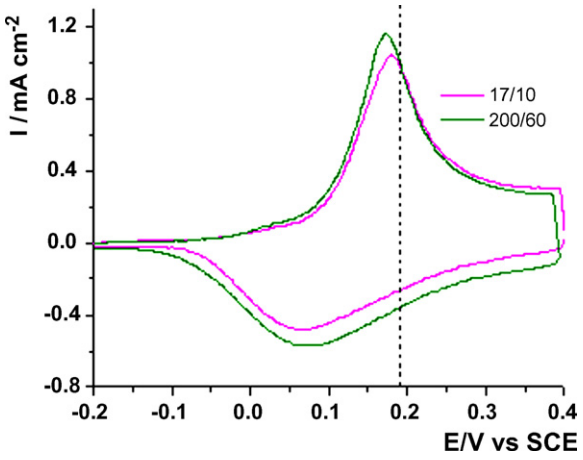

Fig. 1. Cyclic Voltammograms of the 17/10 and 200/60 polyaniline films in monomer free solution (0.5 M H_2SO_4) at $v = 0.05$ mV/s. The dashed line indicates the potential used for the electrodeposition of palladium.

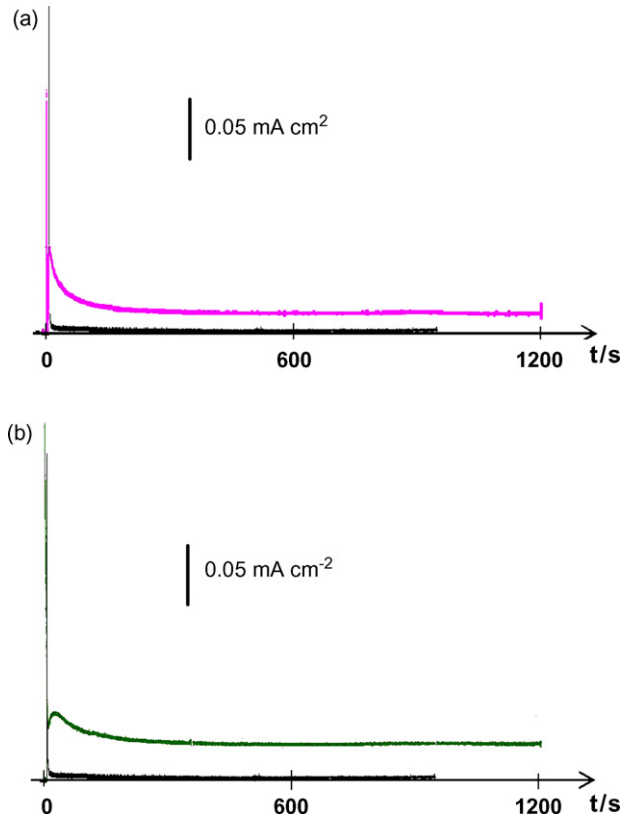

Fig. 2. Chronoamperograms recorded during potential step polarisation of polyaniline films in presence of Pd^{2+} (a) 17/10 and (b) 200/60. Applied potential step +0.400 to +0.190 V vs. SCE. Black curves: chronoamperograms recorded in 0.5 M H_2SO_4.

The thickness of the 17/10 films and 200/60 films was measured by in situ AFM in the oxidised state (+0.400 V versus SCE) and typical values obtained were 107 and 605 nm, respectively.

The chronoamperograms in Fig. 2 are characterized by an initial current decay followed by an ascending part; where a maximum is clearly visible. As expected, the equivalent current transients collected for PAni films in Pd free 0.5 M H_2SO_4 solution (black lines in Fig. 2) only reveal the charging of the polymer matrix.

The main difference observed between the transients of the 17/10 and of the 200/60 films is the position t_m of the current maxima on the time scale, whereby the current maximum is reached after a longer time interval in the case of the 200/60 polymer film. Considering the generally established current–time correlations for 3D nucleation [29–31] the observed increase of t_m may be due to a decrease of the maximum density of nucleation sites and/or a decrease of the growth rate of the individual nuclei. Both properties may be affected by differences in the morphology and thickness of the 17/10 and the 200/60 films. Pronounced morphological differences between the two film types are clearly visible in the previously published SEM images [10] and in the AFM images of Fig. 3: whereas the 17/10 films (Fig. 3a) show a rather compact morphology consisting of small globular features with typical diameters between ca. 20–80 nm, the 200/60 films (Fig. 3b) consist of larger size globules. If the Pd nucleation sites are predominantly located in the contact zones and pores between different globuli of the polymer matrix, a higher site density would indeed be expected for the 17/10 films, and higher pore depths with a slower diffusional supply of Pd^{2+} can be anticipated at the 200/60 films.

In Table 1 the charge associated with the reduction of PAni (Q_{PAni}), was subtracted from the value obtained from the palladium deposition current transient (Q_{mist}), resulting in the deposition charge ($Q_{f\ Pd\ deposition}$). The duration of the potentiostatic Pd deposition was chosen such that the amounts of electrodeposited Pd, quantified by the charge $Q_{f\ Pd\ deposition}$,

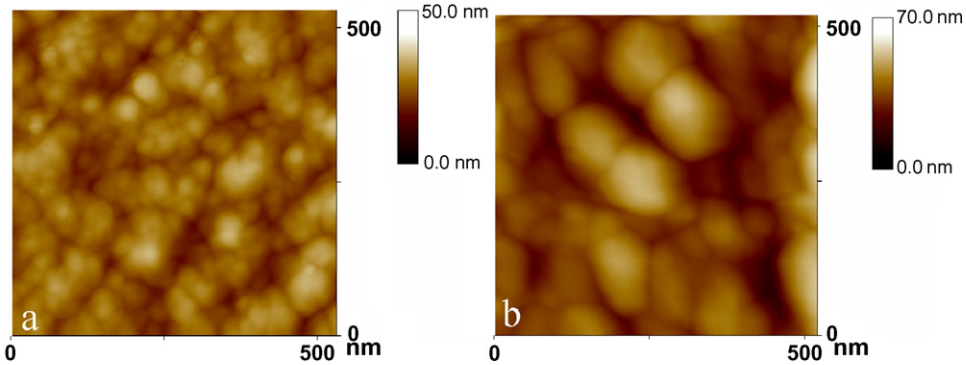

Fig. 3. AFM- tapping mode images of polyaniline films prepared under different polymerisation conditions: (a) 17/10 film, (b) 200/60 film.

Table 1
Deposition time and charges involved in palladium electrodeposition

Film	Deposition time s	Q_{PAni} mC cm^{-2}	Q_{mist} mC cm^{-2}	$Q_{f\ Pd\ deposition}$ $Q_{(mist)} - Q_{(polymer)}$ mC cm^{-2}
17/10	1200	1.43	16.53	15.10
17/10	1860	2.28	35.52	33.24
200/60	1200	1.15	16.42	15.27
200/60	1860	1.91	35.19	33.27

Applied potential step: +0.400 to +0.190 V vs. SCE

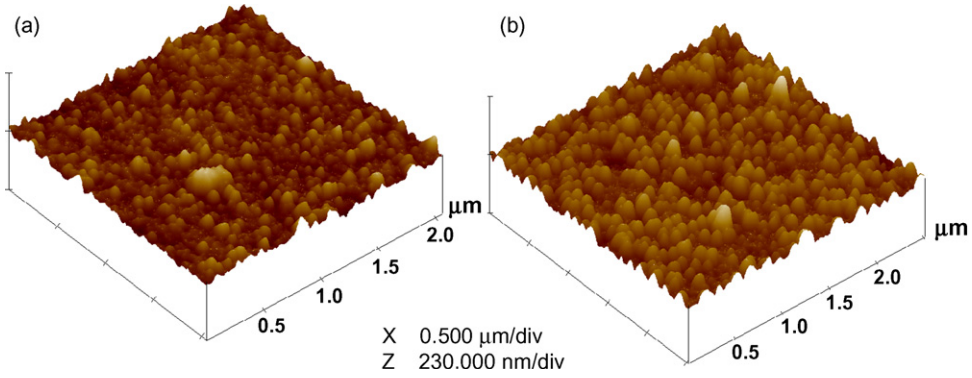

Fig. 4. Ex situ tapping mode AFM images after electrodeposition of Pd onto 17/10 polyaniline films from a solution of 0.001 M $PdSO_4$ in 0.5 M H_2SO_4 by potential step chronoamperometry. Pd deposition by step polarisation from +0.400 to +0.190 V vs. SCE, using deposition times of (a) 1200 s and (b) 1860 s.

equal approximately the amounts of Pd deposited in previous work [10] by electroless deposition at 17/10 and 200/60 films:

15 mC cm^{-2} for electroless deposition during 30 min (17/10/Pd 30 film) and 33 mC cm^{-2} for electroless deposition during 60 min (17/10/Pd60 film).

The morphological characterization of the 17/10 films after electrodepositon during 1200 and 1800 s is presented in Fig. 4, where 3D processed topographic images are shown. Spherical palladium particles are observed and are distributed randomly on the top of the polymer compact layer. Their diameters range

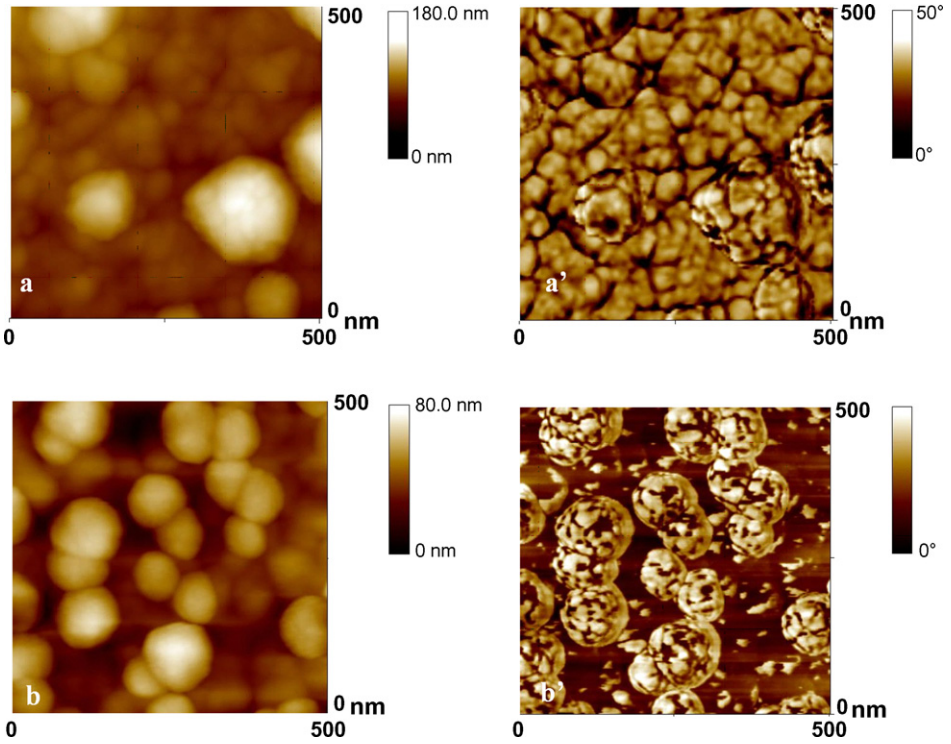

Fig. 5. Ex situ tapping mode AFM images after electrodeposition of Pd onto 17/10 films from a solution of 0.001 M $PdSO_4$ in 0.5 M H_2SO_4 by potential step chronoamperometry. Pd deposition by step polarisation from +0.400 to +0.190 V vs. SCE, using deposition times of (a,a′) 1200 s and (b,b′) 1860 s. (a,b) Topographic images; (a′,b′) phase images. Window size 0.5 µm × 0.5 µm.

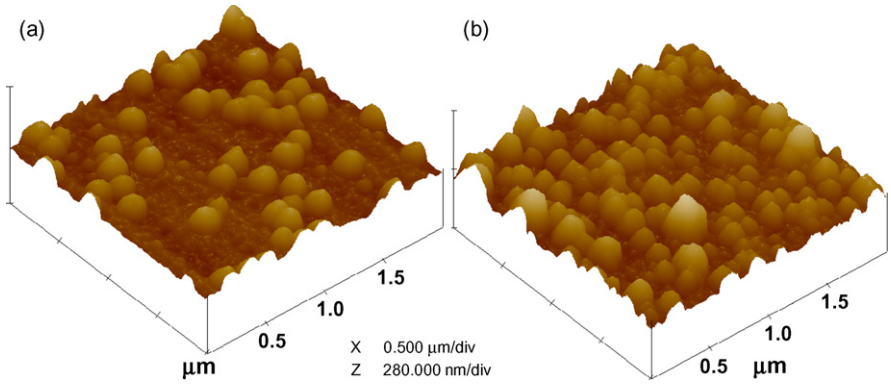

Fig. 6. Ex situ tapping mode topographic AFM images after electrodeposition of Pd onto 200/60 polyaniline films from a solution of 0.001 M $PdSO_4$ in 0.5 M H_2SO_4 by potential step chronoamperometry. Pd deposition by step polarisation from +0.400 to +0.190 V vs. SCE, using deposition times of (a) 1200 s and (b) 1860 s.

from ca. 50 to ca. 90 nm after 1200 s deposition time (Fig. 4a), increasing to ca. 100 nm with time of deposition (Fig. 4b). In Fig. 5 higher magnification topographic and phase images are displayed, where the palladium clusters are clearly recognised.

Fig. 6 shows 3D processed ex situ topographic AFM images of 200/60 polyaniline films after potential step deposition of Pd during 1200 s (Fig. 6a) and 1860 s (Fig. 6b). The observed palladium clusters are distributed on the surface of the polyaniline film and upon extension of the deposition time, additional small cluster features appear in the phase-mode image, and the number density appears to increase compared to the value obtained with 1200 s. A possible explanation for this observation is the visualization of additional particles that were previously formed in micropores inside the film matrix [1,2], or even at the polyaniline/Au interface: these can only be visualized as the surface film domains by the (surface-confined) phase-mode AFM technique after growing into those layers during the extended deposition times. Fig. 7 shows enlarged topographic and phase images (0.5 µm × 0.5 µm) of the Pd modified polymer, where it is possible to distinguish Pd particles with diameters of approximately 10 nm which are part of the Pd clusters observed.

The results described above and in [10] clearly show that the deposition method for embedding palladium particles on polyaniline films, plays an important role on the amount and

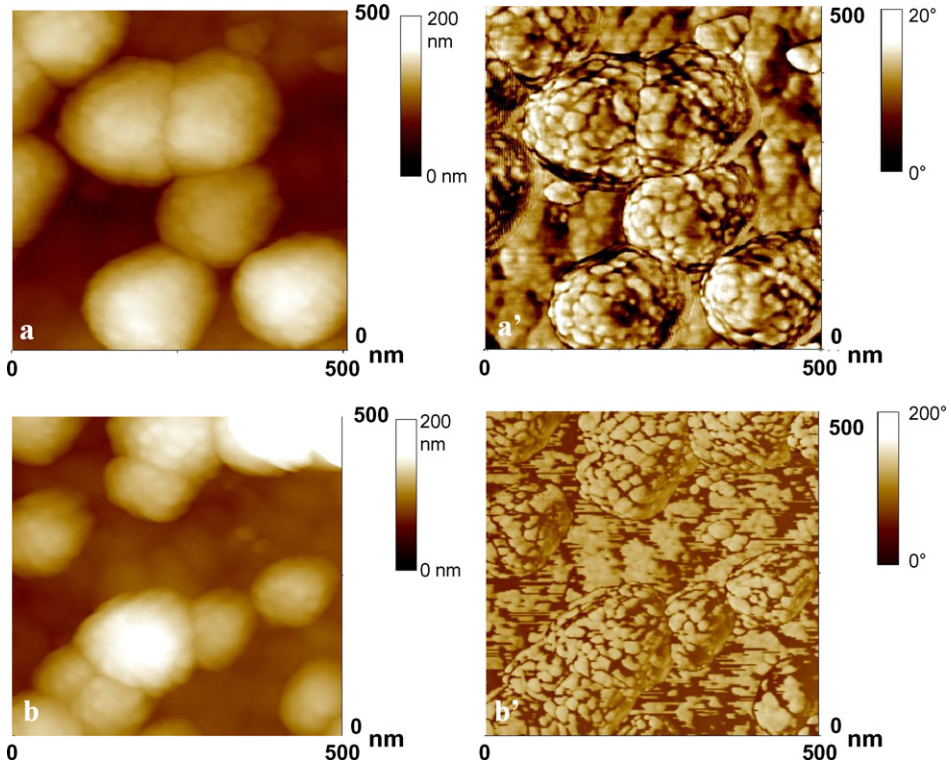

Fig. 7. Ex situ tapping mode AFM images after electrodeposition of Pd onto 200/60 polyaniline films from a solution of 0.001 M $PdSO_4$ in 0.5 M H_2SO_4 by potential step chronoamperometry. Pd deposition by step polarisation from +0.400 to +0.190 V vs. SCE, using deposition times of (a,a′) 1200 s and (b,b′) 1860 s. (a,b) Topographic images; (a′,b′) phase images.

distribution of the metallic clusters. In general the electroless precipitation of palladium on the 17/10 film leads to the formation of particles distributed in a non-uniform arrangement on the top of the polymer layer whose diameter ranges from 20–30 nm and from 80 to 290 nm, if the process occurred for 1800 and 3600 s, respectively. Also the amount of metallic particles increased with the time deposition. In the 200/60 film the palladium clusters could not be clearly distinguished from the polymer features in the topographic AFM images, although the globules exhibit smaller clusters (diameter 15–20 nm) covering their surface and were much more clearly visualized in a smaller scale phase image. As additional criterion for the discrimination between polymer globules and Pd particles in the AFM images, increasing Pd deposition time could be associated on both films with a slight enlargement of clustered features that obviously represent Pd deposits. For example, after deposition of palladium for 1200 s the 17/10 film presents clusters with diameters ranging from 50 to 90 nm, whereas after 1860 s the diameters increase to 100 nm. On the 200/60/Pd modified electrode, a similar behaviour was observed, where an increase of the diameter of the palladium clusters from 100 to 120 nm was recorded. Moreover, the number density of the metallic particles synthesised by this deposition method is much higher than that observed by electroless precipitation.

3.2. Influence of the potential step duration on size and distribution of Pd particles electrodeposited at the 200/60 polyaniline films

Further potential step polarization experiments (stepping from +0.400 to +0.190 V versus SCE) were performed at 200/60 films using different step durations of 5, 15 and 30 s, followed by ex situ AFM investigations of the resulting Pd/polyaniline composite films, as illustrated by Fig. 8. The Pd nanoparticles are visible in the phase-mode AFM images as small patterns with enhanced brightness due to their different viscoelastic properties with respect to the polyaniline film matrix. For short deposition times, i.e. up to 30 s, the average Pd particle diameters and number densities were evaluated by counting the number of visible clusters at different scan window sizes and are listed in Table 2.

As can be seen in Fig. 8 and from the data in Table 2, an extension of the deposition time from 5 to 15 s not only results in larger diameters of the particles, but also in a considerable increase of the particle number density. This is an indication that, in the deposition range between 5 and 15 s, still additional particles are formed, in contrast to the limiting model of instantaneous nucleation. Upon further extension of the deposition time from 15 to 30 s, the observed particle number density remains practically constant, but the particles grow to average sizes around 40 nm, where they are close to mutual contact. The substantial increase of the deposition time to 1200 s results in a rather compact appearance of the Pd coverage (Fig. 6a) combined with a considerable decrease of the number density (Table 2). These observations are most likely due to a substantial amount of coalescence of individual particles by the extended growth into larger clusters. For this reason, the number density value is in brackets in Table 2, as it should not be considered a real quantity.

This would also imply that the particles observed in Fig. 8 after short deposition times, are essentially particles at the surface or in the superficial layer of the polymer matrix.

Table 2
Diameters and number densities of Pd particles electrodeposited on 200/60 polyaniline films

Deposition time s	N particles/cm^2	Particle diameter (nm)	
		Average diameter	Diameter range
5	1.80×10^6	8.6	6.4–10.7
15	4.29×10^6	18.0	12.8–23.7
30	4.22×10^6	39.1	15.6–62.5
1200[a]	(3.8×10^6)[a]	116.1[a]	47.5–184.6[a]
1860[a]	(8.7×10^6)[a]	109.8[a]	44.7–174.9[a]

The values are determined from AFM images
[a] See restrictions mentioned in the preceding text for the significance of the values for the deposition times 1200 and 1860 s.

3.3. Nucleation and growth mechanism of the Pd particles on the 200/60 films

A first appraisal on the nucleation and growth mechanism of the Pd particles on the PAni films was performed by comparison of the experimental cathodic current transients of Pd electrodeposition with the theoretical plots for different types of nucleation. Taking into account the requirement of a well defined nucleation peak at the initial moments of deposition, for this study, the electrodeposition of Pd in/on the polymer films was studied in the potential range between 0.120 and 0.190 V versus SCE (Fig. 9). Also, if the transients recorded for the PAni film in absence of Pd deposition (Fig. 9, inset) are subtracted from the transients obtained during Pd deposition, the resulting difference transients (Fig. 10) with a current maximum exhibit the typical features of a metal deposition process controlled by nucleation and growth [7–9], in particular when the potential was stepped to +0.120 V.

The families of chronoamperograms in Fig. 9 are characterised by an initial current decay followed by an ascending part and for steps to 0.150 and 0.120 V a maximum is clearly visible. As expected, the equivalent current transients collected for PAni films in Pd free 0.5 M H_2SO_4 solution (inset in Fig. 9) only reveal the charging of the polymer matrix. Following early theoretical concepts for electrochemical nucleation [30], the theoretical treatment of potential step chronoamperometry for multiple nucleation with diffusion-controlled growth has been the subject of detailed studies by various groups [31–36].

According to Scharifker et al. [31,32], dimensionless equations can be used for metallic deposits formed by nucleation and growth in three-dimensional matrixes (e.g. polymers) of limited thickness [15], to compare the experimentally observed nucleation process with the two limiting cases of instantaneous and progressive nucleation, and to discriminate between two- or three-dimensional growth. While in the model of Scharifker et al. the diffusion layer thickness used for the calculation of the

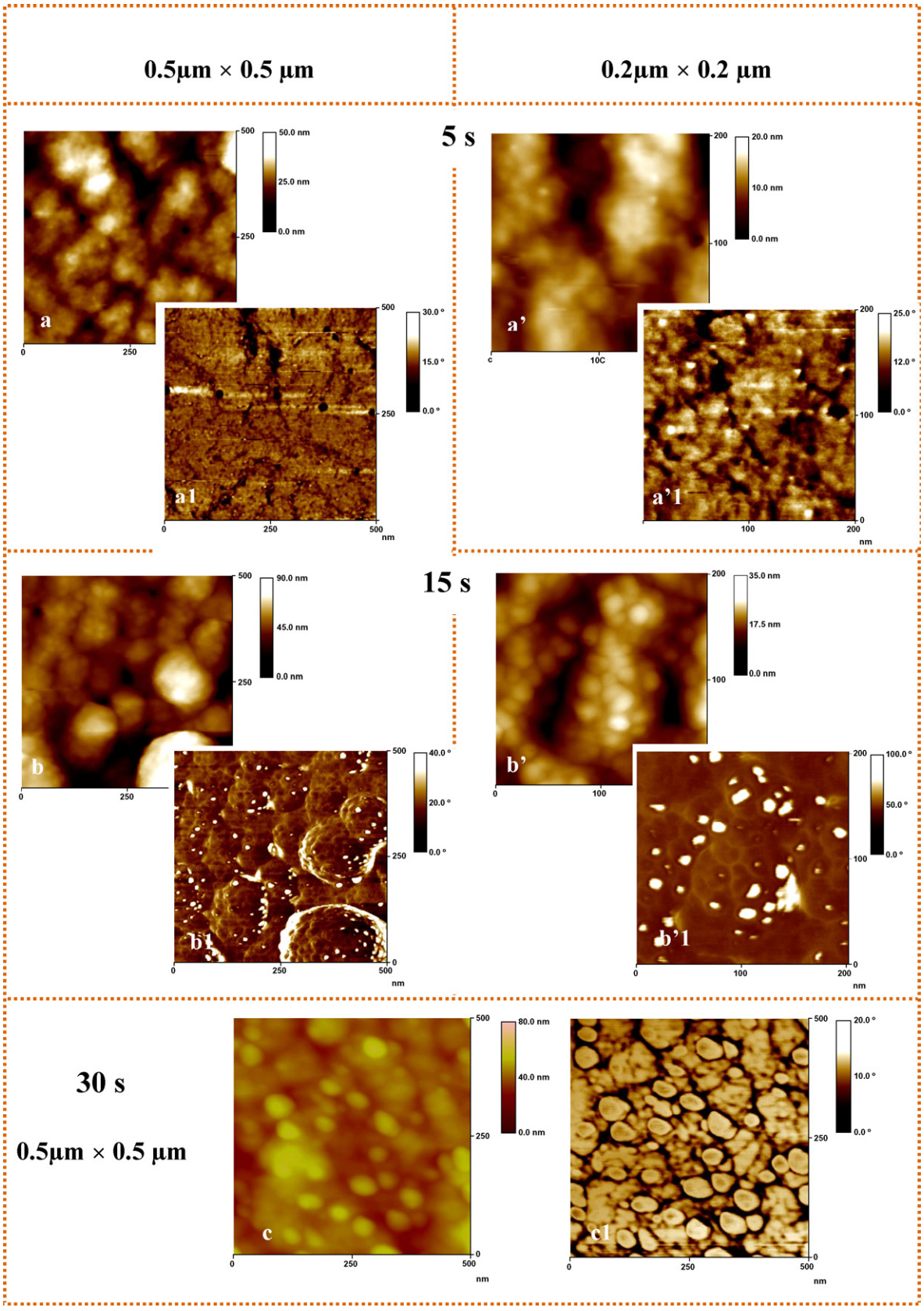

Fig. 8. Electrodeposition of Pd onto 200/60 polyaniline films from a solution of 0.001M $PdSO_4$ in 0.5 M H_2SO_4 by potential step chronoamperometry. Pd deposition by step polarisation from +0.400 to 0.190 V vs. SCE, using short deposition times of 5 s (a), 15 s (b) and 30 s (c). The tapping mode AFM chracterization of the Pd deposits was carried out ex situ in the topographic mode and in the phase mode. (a, a′, b, b′, c) Topographic images; (a1, a′1, b1,b′1, c1) phase images.

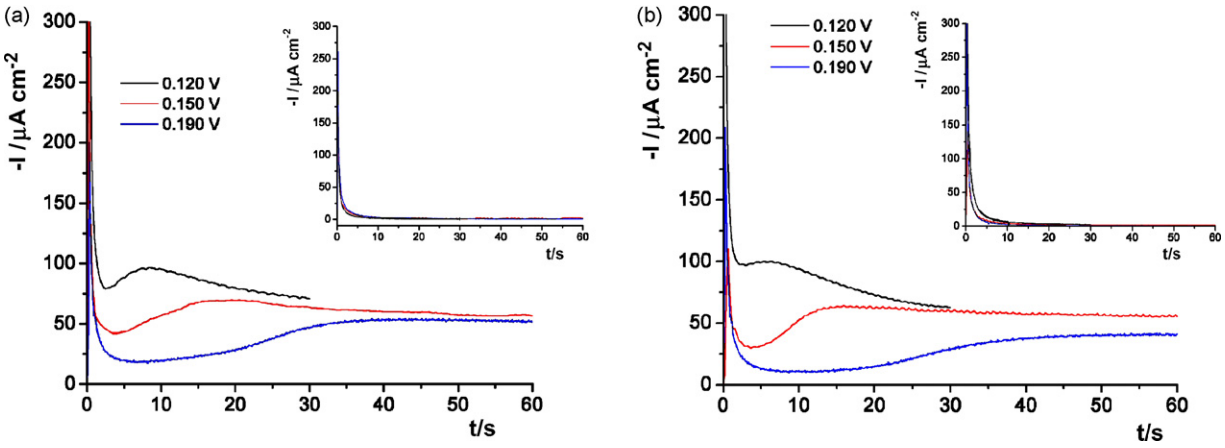

Fig. 9. Chronoamperograms recorded during potential step polarisation of polyaniline films in presence of Pd^{2+} in 0.5 M H_2SO_4 + 0.001 M $PdSO_4$. (a) 17/10 films and (b) 200/60 films. Applied potential step +0.400 to +0.120, +0.150 and +0.190 V vs. SCE. Insets: chronoamperograms recorded in 0.5 M H_2SO_4.

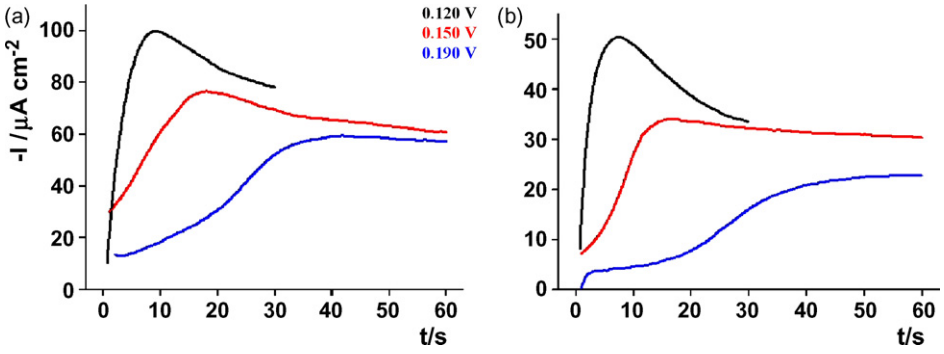

Fig. 10. Corrected potential step chronoamperograms obtained in presence of Pd^{2+} in 0.5 M H_2SO_4 +0.001 M $PdSO_4$. The chronoamperograms have been corrected by subtraction of the corresponding chronoamperograms recorded in Pd-free 0.5 M H_2SO_4. (a) 17/10 films and (b) 200/60 films. Applied potential steps +0.400 to +0.120, +0.150 and +0.190 V vs. SCE.

current densities only depends on the time, a modified model has been presented by Heerman and Tarallo [35,36], where the diffusion layer thickness also depends on the nucleation rate constant.

Fig. 11 presents experimental dimensionless plots of $(I/I_m)^2$ versus (t/t_m) for the electrodeposition of palladium at +0.120 V on the two different PAni films; also shown are the theoretical curves corresponding to the limiting cases for instantaneous and progressive nucleation for a 3D growth. It has been shown [35,36] that these theoretical curves for instantaneous and progressive nucleation coincide for the two models by Scharifker et al. and by Heerman and Tarallo.

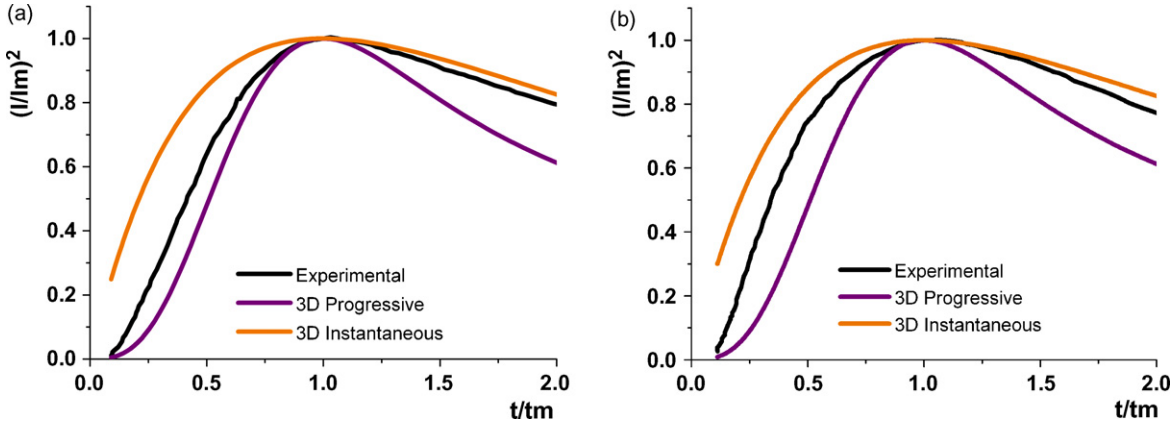

Fig. 11. Plot of the dimensionless quantity $(I/I_m)^2$ vs. (t/t_m) [30,31] for the palladium electrodeposition at +0.120 V vs. SCE on the different polyaniline films. Comparison of the experimental results (for potential step polarisation from +0.400 to +0.120 V vs. SCE) with the theoretical results for 3D instantaneous and progressive nucleation and growth, (a) 17/10/Pd and (b) 200/60/Pd.

On both films, the data of Fig. 11 show clearly that the experimental transients neither coincide with the progressive nor with the instantaneous nucleation scheme, but fall between these two limiting cases. These results differ from a previous study of Pd electrodeposition on polyaniline films by Leone et al. [19], where the experimental results closely coincide with the limiting case of instantaneous nucleation. A possible explanation for the different results obtained in our work might be due to the distinct morphology of the polyaniline films since the polymers reported in [19] were grown galvanostatically and the Pd deposition was carried out onto polyaniline in its reduced state, i.e., at potentials where the film is electronically insulating in contrast with the experiments described in the present work where it is reported the palladium deposition on PAni at potentials where it is in the conducting state.

4. Conclusions

Applying a pulse potential from +0.400 to +0.190 V it is possible to incorporate Pd particles on potentiodynamically synthesized PAni. The different morphologies of the films affect the current transient features, namely the position of the current maxima on the time scale (longer lapse for 200/60).

A decrease of the maximum density of nucleation sites was obtained for the film displaying larger sized globules (200/60) as well as a slower diffusional supply of Pd^{2+} with concomitant decrease of the growth rate of individual nuclei.

A detailed study of potential step electrodeposition on the more porous polymer matrix using different deposition times in combination with ex situ phase-mode AFM visualization of the resulting Pd/polyaniline composites suggests that a constant number density of critical Pd nuclei is reached in the superficial parts of the film matrix within ca. 15 s, indicating that the electrodeposition of the Pd particles does not follow an instantaneous nucleation mechanism, as is also confirmed by a quantitative evaluation of the current density transients. The achieved constant number density of the particles in the superficial parts of the polymer may be imposed by the density of special nucleation sites in the superficial polymer matrix, e.g. grain boundaries or micropores between polymer globules. Additional Pd nuclei that are considered to be formed initially also in the internal porous domains of the polymer matrix or even at the polymer/Au interface are presumably not imaged initially by the phase-mode AFM technique, but are only detected after their growth into the superficial parts of the polymer during more extended deposition times. The results illustrate the high potential of the AFM phase-mode technique for the visualization of hard nanometer-size particles in the superficial part of a soft polymer matrix, but show also the limitation of this method for the particle visualization in the polymer bulk.

The electrodeposition method provides a better control of the size of the Pd clusters than the electroless precipitation, where different sized Pd nuclei were observed even in the same modified electrode.

Acknowledgments

The authors acknowledge Dr. A. S. Viana for the AFM imaging, Laboratório de SPM, Faculdade de Ciências, Universidade de Lisboa.

This work was financially supported by Fundação para a Ciência e a Tecnologia, through Ph.D. scholarship PRAXIS XXI/BD 21424/99.

References

[1] A. Frydrychewicz, S.Y. Vassiliev, G.A. Tsirlina, K. Jackowska, Electrochim. Acta 50 (2004) 1885.
[2] L.M. Abrantes, J.P. Correia, Electrochim. Acta 45 (2000) 4179.
[3] M. Musiani, Electrochim. Acta 45 (2000) 3397.
[4] A.M.C. Luna, J. Appl. Electrochem. 30 (2000) 1137.
[5] L.H. Mascaro, D. Gonçalves, L.O.S. Bulhões, Thin Solid Films 461 (2004) 243.
[6] A. Drelinkiewicz, M. Hasik, J. Mol. Catal. A: Chemical 177 (2001) 149.
[7] A.A. Mikhaylova, E.B. Molodkina, O.A. Khazova, V.S. Bagotzky, J. Electroanal. Chem. 509 (2001) 119.
[8] J. Wang, K.G. Neoh, E.T. Kang, J. Colloid Interface Sci. 239 (2001) 78.
[9] G. Wu, L. Li, J.H. Li, B.Q. Xu, Carbon 45 (2005) 2579.
[10] A. Mourato, A.S. Viana, J.P. Correia, H. Siegenthaler, L.M. Abrantes, Electrochim. Acta 49 (2004) 2249.
[11] A. Mourato, S.M. Wong, H. Siegenthaler, L.M. Abrantes, J. Solid State Electrochem. 10 (2006) 140.
[12] L. Niu, Q. Li, F. Wei, S. Wu, P. Liu, X. Cao, J. Electroanal. Chem. 578 (2005) 331.
[13] C. Coutanceau, M.J. Croissant, T. Napporn, C. Lamy, Electrochim. Acta 46 (2000) 579.
[14] M.J. Giz, S.L.A. Maranhão, R.M. Torresi, Electrochem. Commun. 2 (2000) 377.
[15] L. Niu, Q. Li, F. Wei, X. Chen, H. Wang, Synth. Met. 139 (2003) 271.
[16] S. Lissy, G. Leinad, S. Pitchumani, K. Jayakumar, Mater. Chem. Phys. 76 (2002) 143.
[17] C.H. Yang, T.C. Wen, Electrochim. Acta 44 (1998) 207.
[18] Y.M. Maksimov, E.A. Kolyadko, A.V. Shishlova, B.I. Podlovchenko, Russ. J. Electrochem. 37 (2001) 777.
[19] A. Leone, W. Marino, B.R. Sharifker, J. Electrochem. Soc. 139 (1992) 438.
[20] M. Hasik, A. Drelinkiewicz, E. Wenda, Synth. Met. 119 (2001) 335.
[21] A. Drelinkiewicz, M. Hasik, M. Kloc, Catal. Lett. 64 (2000) 41.
[22] L.M. Abrantes, J.P. Correia, Mater. Sci. Forum 191 (1995) 235.
[23] V. Tsakova, S. Winkels, J.W. Schultze, J. Electroanal. Chem. 500 (2001) 574.
[24] J.M. Ortega, Thin Solid Films 360 (2000) 159.
[25] S. Ivanov, V. Tsakova, Electrochim. Acta 50 (2005) 5616.
[26] B.J. Hwang, R. Santhanam, Y.L. Lin, Electroanalysis 15 (2003) 1667.
[27] V. Tsakova, D. Borissov, B. Ranguelov, Ch. Stromberg, J.W. Schultze, Electrochim. Acta 46 (2001) 4213.
[28] N. Hernández, J.M. Ortega, M. Choy, R. Ortiz, J. Electroanal. Chem. 515 (2001).
[29] A.E. Alvarez, D.R. Salinas, J. Electroanal. Chem. 566 (2004) 393.
[30] J.A. Harrison, H.R. Thirsk, in: A.J. Bird (Ed.), Electroanalytical Chemistry, vol. 5, Marcel Dekker, New York, 1971.
[31] B. Sharifker, G. Hills, Electrochim. Acta 28 (1983) 879.
[32] B.R. Scharifker, J. Mostany, J. Electroanal. Chem. 177 (1984) 13.
[33] M. Sluyters-Rehbach, J.H.D.J. Wijenberg, E. Bosco, J. Sluyters, J. Electroanal. Chem. 236 (1987) 1.
[34] M.V. Mirkin, A.P. Nilov, J. Electroanal. Chem. 283 (1990) 35.
[35] L. Heerman, A. Tarallo, J. Electronanal. Chem. 470 (1999) 70.
[36] L. Heerman, A. Tarallo, Electrochem. Commun. 2 (2000) 85.